Applied Catalysis B: Environmental 100 (2010) 157–164

Contents lists available at ScienceDirect

Applied Catalysis B: Environmental

journal homepage: www.elsevier.com/locate/apcatb

Direct ethanol fuel cells: The effect of the cell discharge current on the products distribution

G. Andreadis [a], V. Stergiopoulos [a], S. Song [b], P. Tsiakaras [a,*]

[a] Department of Mechanical Engineering, School of Engineering, University of Thessaly, Pedion Areos, 383 34 Volos, Greece
[b] State Key Laboratory of Optoelectronic Materials and Technologies, School of Physics and Engineering, Sun Yat-Sen University, Guangzhou 510275, China

ARTICLE INFO

Article history:
Received 12 May 2010
Received in revised form 18 July 2010
Accepted 22 July 2010
Available online 30 July 2010

Keywords:
Direct ethanol PEM fuel cell
On-line product analysis
Ethanol conversion
Products distribution

ABSTRACT

In the present work the results of the continuous and on-line product analysis during a Direct Ethanol Polymer Electrolyte Membrane Fuel Cell operation (DE-PEMFC) are presented. The effect of both cell discharge current and operating temperature on (a) the ethanol's conversion, (b) the reaction products distribution and (c) the reaction yield towards each released product, is examined. The MEA used during the experiments is comprised of a PtRu/C anode, a Nafion®-115 membrane and a Pt/C cathode. It is found that the increase of the cell current and the operating temperature lead to an increase of the ethanol conversion. The maximum ethanol conversion is found to be 4.6% and it is recorded when the cell current is 120 mA and the cell temperature is 90 °C. The main products detected during the fuel cell operation are acetaldehyde (CH_3CHO), acetic acid (CH_3COOH) and small amounts of carbon dioxide (CO_2). The selectivity of acetaldehyde ranges from 45% to 70%, the selectivity of acetic acid ranges from 25% to 45% and the selectivity of CO_2 ranges from 5% to 15%. As it concerns the reaction yield towards each product, it is found that the increase of the temperature results in an increase of the yield. Furthermore, from the Arrhenius plots based on the products formation rate, it is found that the acetaldehyde is favored over PtRu/C compared to the other products. Finally, based on the apparent activation energy of the CO_2 formation rate (50 kJ mol^{-1}), it is concluded, that the C–C bond breakage of the ethanol molecule is difficult to occur over the anode catalyst.

1. Introduction

Direct ethanol proton exchange membrane fuel cells (DE-PEMFCs) are promising candidates as power sources especially in small-scale applications. The last decade polymer electrolyte membrane fuel cells (PEMFCs) directly fed by ethanol have been receiving more and more attention, due to the fuel advantages [1,2]. However, there are some challenges that should be overcome, such as: (i) the high anode overpotential values, (ii) the ethanol crossover from the anode to the cathode side of the cell and (iii) the poisoning of the cathode catalysts due to the parasitic oxidation of ethanol, which leads to the mixed potential formation.

Over the last years, several experimental works have been devoted to the direct use of ethanol in fuel cells [1,2]. Almost all these scientific works deal with the problem of the slow ethanol electro-oxidation kinetics at the anode compartment, and the research conducted to find more effective catalysts [3–27]. In order to effectively examine the role of a catalyst and the ethanol reaction mechanism over this catalyst, the analysis of the released products during the ethanol oxidation should be performed. The methodology used for the products analysis during a DE-PEMFC operation is thoroughly discussed and reported in the literature [14,20]. Moreover, in situ infrared reflection–absorption spectroscopy [28,29] and differential electrochemical mass spectrometry [30] have been successfully used for the products identification during the ethanol electro-oxidation in acid medium over Pt and Pt-based electrocatalysts. In the above-mentioned studies, the main products detected during the ethanol oxidation were acetaldehyde, acetic acid and CO_2. Each product yield was dependent on the experimental conditions.

In the present work, for the sake of on-line qualitative and quantitative analysis of the products from ethanol oxidation, a combined approach for the continuous and on-line products analysis during the DE-PEMFC operation is presented. More precisely, the analysis of ethanol's electro-oxidation reaction products is performed in a specially designed experimental apparatus, which combines a gas chromatograph (GC), a mass spectrometer (MS) and three IR gas analyzers. The main advantages of the present method are: (i) the products analysis is performed on-line in real time during the DEFC operation, in contrast to the methodology adopted in other works; in which the mixture of the released products was trapped in different bottles before being analysed, (ii) the continuous and on-line

* Corresponding author. Tel.: +30 24210 74065; fax: +30 24210 74050.
E-mail address: tsiak@mie.uth.gr (P. Tsiakaras).

0926-3373/$ – see front matter © 2010 Elsevier B.V. All rights reserved.
doi:10.1016/j.apcatb.2010.07.025

analysis could provide information about the reaction behavior as well as the whole phenomena occurring during the fuel cell tests, and (iii) the continuous and on-line analysis reduces the possible experimental errors. This is due to the fact that in the case of sample collections, the mixture of the released products trapped in different bottles contains extremely volatile substances, such as acetaldehyde.

2. Experimental

2.1. Catalysts and MEA preparation

The Pt/C and PtRu/C electrocatalysts were fast and easily prepared by a pulse-microwave assisted polyol synthesis method [31]. The primary steps of this synthesis process are given as follows: in a beaker, the starting precursors were well mixed with ethylene glycol (EG) in an ultrasonic bath, and then XC-72 R carbon black was added into the mixture. After the pH value of the system was adjusted to more than 10 by the drop-wise addition of 1.0 mol L^{-1} NaOH/EG, a well-dispersed slurry was obtained with ultrasonic stirring for 30 min. Thereafter, the slurry was microwave-heated in the pulse form with every 5 s for several times. In order to promote the adsorption of the suspended metal nanoparticles onto the support, hydrochloric acid was adopted as the sediment. After that, the resulting black solid sample was filtered, washed, and dried at 80 °C overnight in a vacuum oven. The obtained PtRu/C and Pt/C were used as the anode and cathode catalyst, respectively. Nafion®-115 membrane was adopted as the electrolyte. The membrane electrode assembly (MEA) was prepared in the same procedure as reported before and its surface is 4 cm^2 [32]. The respective metal loading for the anode and cathode was 2.0 and 2.5 mg Pt cm^{-2}. The TEM image of the as-prepared PtRu catalyst and the histogram of the PtRu particles size distribution is presented in Fig. 1(a) and (b), respectively.

2.2. Experimental apparatus

The schematic representation of the experimental apparatus used during the experiments is shown in Fig. 2. The ethanol aqueous solution was fed to the anode compartment at a flow rate of 0.5 ml min^{-1} by the aid of a dual syringe pump. The ethanol concentration was 1.0 mol L^{-1}. Consequently, the amount of ethanol fed to the anode was 5×10^{-4} mol min^{-1}. The ethanol aqueous solution before entering the anode was preheated at the cell temperature. The pressure at both anode and cathode sides was equal to the atmospheric one. The volumetric flux of oxygen was controlled via mass flow controllers. The oxygen before entering the cathode was humidified and preheated at the cell temperature. All the single fuel cell tests were performed using an AMEL-5000 electrochemical station. The products released during the ethanol electro-oxidation over the anode catalyst were driven in a stainless steel bottle, which was used as an evaporator. The bottle was heated to the high temperature of ~200 °C, which was used to guarantee the thorough gasification of the released liquid mixture including water, ethanol oxidation products and the unreacted ethanol. The gasification of the products is compulsory due to the fact that the analysis system consists of a gas chromatograph Shimadzu GC-14B, equipped with a Porapak QS column, a mass spectrometer Omnistar-Balzers and three gas analysers (Hartmann & Braun). The capacity of the evaporator was about 1 L. This gasification operating temperature was determined via a series of blank experiments; in order to be sure that the evaporator's working temperature is not enough for the ethanol's homogeneous activation. It is worthy to be noticed that all the lines of the experimental apparatus were stainless steel tube (1/8 in. in diameter) and they were heated via heating tapes at 140 °C in order to avoid the condensation of the gasified products mixture.

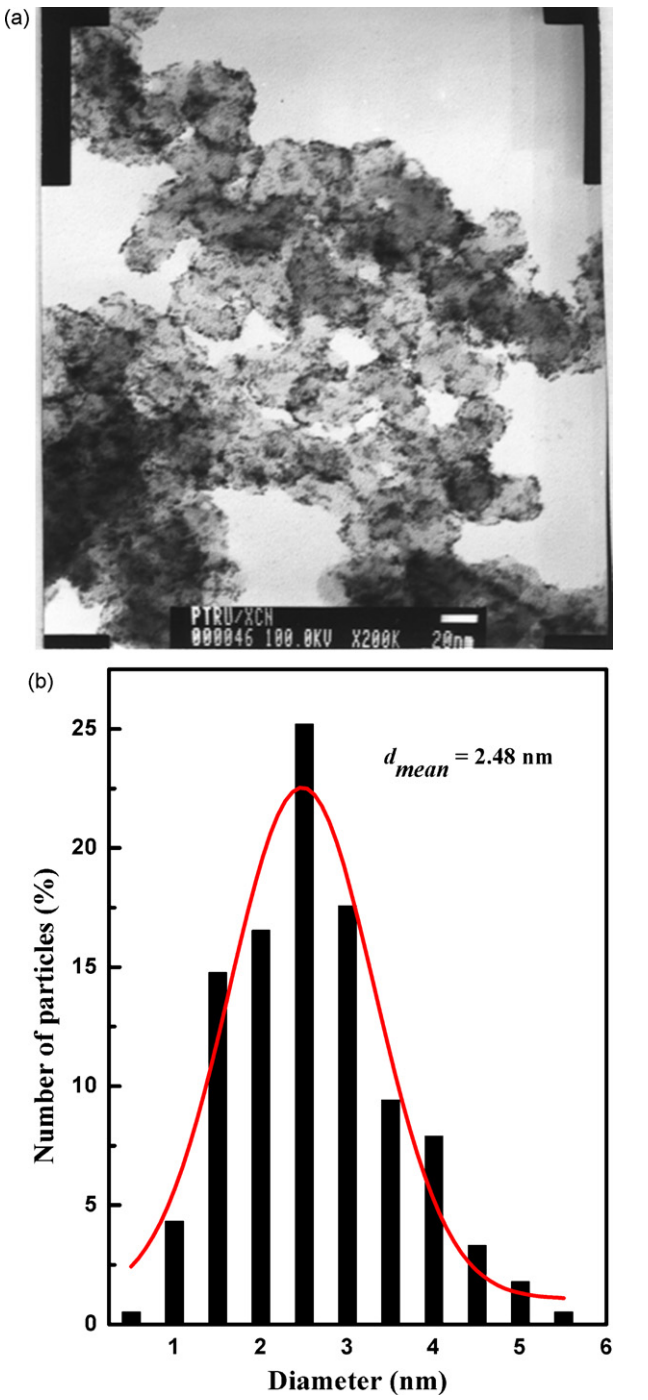

Fig. 1. (a) TEM image of the as-prepared PtRu catalyst and (b) histogram of the PtRu particles size distribution.

2.3. Calculation of ethanol conversion, products selectivity and yield

In this paragraph, the equations used for the calculation of ethanol conversion, products selectivity and the reaction yield towards each product formation are presented. More precisely, the ethanol conversion is calculated from Eq. (1):

$$X_{EtOH} = \frac{(0.5 \times CO_2 + CH_3CHO + CH_3COOH) \times \dot{V}_{out}}{(EtOH_{in} - EtOH_{cross}) \times \dot{V}_{in}} \times 100 \qquad (1)$$

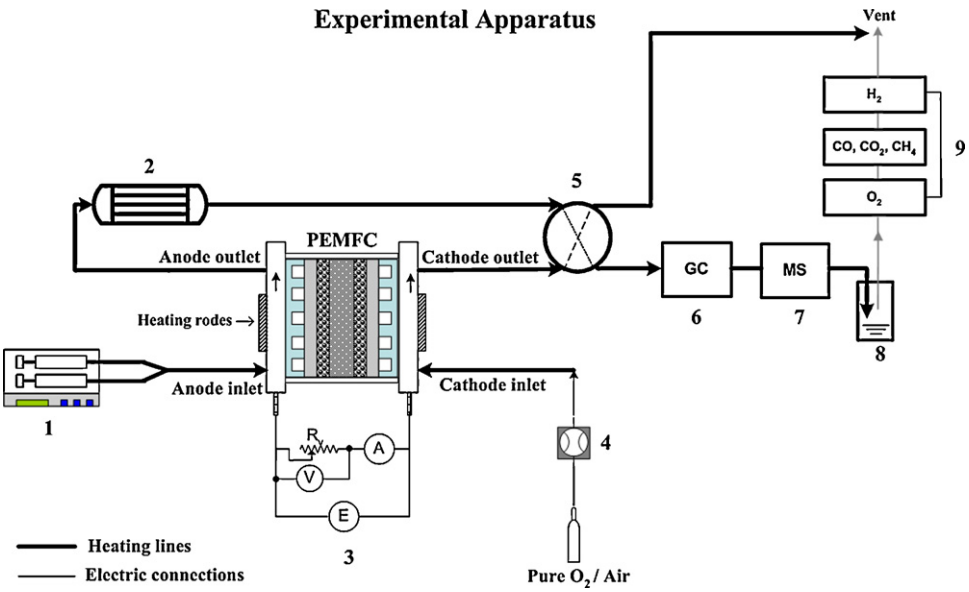

Fig. 2. Schematic representation of the experimental apparatus. 1: Dual syringe pump, 2: Evaporator, 3: Electrochemical Test Station AMEL, 4: Mass flow controllers, 5: Four-way valve, 6: Gas chromatograph, 7: Mass spectrometer, 8: Condensator, 9: Gas analyzers.

where $EtOH_{in}$ is the ethanol feed concentration, $EtOH_{cross}$ is the crossovered ethanol concentration, CO_2, CH_3CHO and CH_3COOH are the concentrations of the released products, and V_{out} and V_{in} are the volume fluxes at the inlet and the outlet of the anode.

The released products during the cell operation are acetaldehyde, acetic acid and CO_2 and they are formed according to the following reactions:

$$CH_3CH_2OH \rightarrow CH_3CHO + 2H^+ + 2e^- \quad (r1)$$

$$CH_3CH_2OH + H_2O \rightarrow CH_3COOH + 4H^+ + 4e^- \quad (r2)$$

$$CH_3CH_2OH + 3H_2O \rightarrow 2CO_2 + 12H^+ + 12e^- \quad (r3)$$

The selectivity of each product is calculated according to the following equations:

$$S_{CH_3CHO} = \frac{(CH_3CHO) \times \dot{V}_{out}}{(0.5 \times CO_2 + CH_3CHO + CH_3COOH) \times \dot{V}_{out}} \times 100 \quad (2)$$

$$S_{CH_3COOH} = \frac{(CH_3COOH) \times \dot{V}_{out}}{(0.5 \times CO_2 + CH_3CHO + CH_3COOH) \times \dot{V}_{out}} \times 100 \quad (3)$$

$$S_{CO_2} = \frac{(0.5 \times CO_2) \times \dot{V}_{out}}{(0.5 \times CO_2 + CH_3CHO + CH_3COOH) \times \dot{V}_{out}} \times 100 \quad (4)$$

where CO_2, CH_3CHO and CH_3COOH are the product concentrations, and V_{out} is the volumetric flux at the anode outlet.

The reaction yield towards each product is calculated via Eqs. (5)–(7):

$$Yield_{CH_3CHO} = X_{EtOH} \times S_{CH_3CHO} \quad (5)$$

$$Yield_{CH_3COOH} = X_{EtOH} \times S_{CH_3COOH} \quad (6)$$

$$Yield_{CO_2} = X_{EtOH} \times S_{CO_2} \quad (7)$$

3. Results and discussion

3.1. Single direct ethanol fuel cell performance

In Fig. 3 the polarization curves *V–I* and *P–I* during the DEFC operation at four different temperatures are depicted. The cathode side of the cell was fed with pure oxygen at a flow rate of 50 ml min^{-1}. As it can be seen from the figure, the increase of the temperature leads to an enhanced cell performance, which is due to the obvious reason that the higher temperature can improve the electrode reaction kinetics. The effect of the operating temperature on the cell maximum power density is illustrated in the inset of Fig. 3. It can be seen that the maximum power density is enhanced approximately by 200% as the temperature increases from 60 to 90 °C.

3.2. Galvanostatic (discharge) operation of the cell

In order to perform the on-line analysis of the products released during the cell operation, the cell was operated galvanostatically at a constant current value for a few hours. For this purpose, the cell was operated at four different cell current values and four different temperatures according to the following criteria: (i) the cell voltage should not be lower than 0.1 V, in order to avoid the deep discharge of the cell and (ii) the temperatures should not exceed the temperature limit that Nafion®-115 membrane can work effectively ($T \leq 90$ °C). More precisely, the cell should be operated at a constant discharge current and temperature for a few hours. During

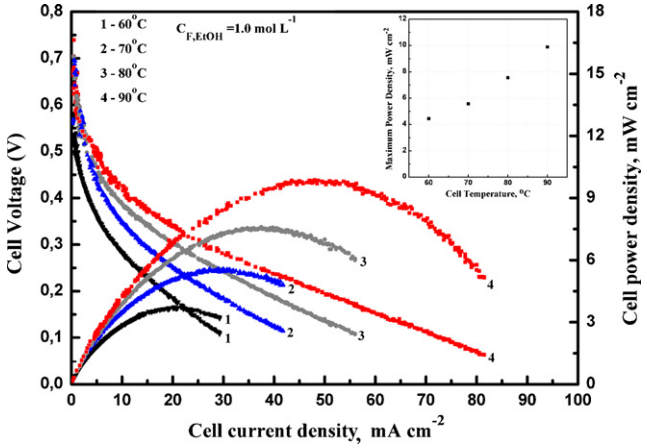

Fig. 3. Polarization curves (*V–I*) and (*P–I*) during the cell operation at different temperatures. Anode: ethanol feed concentration is 1.0 mol L^{-1}, volumetric flow rate is 0.5 ml min^{-1}. Cathode: pure oxygen humidified, volumetric flow rate 50 ml min^{-1}.

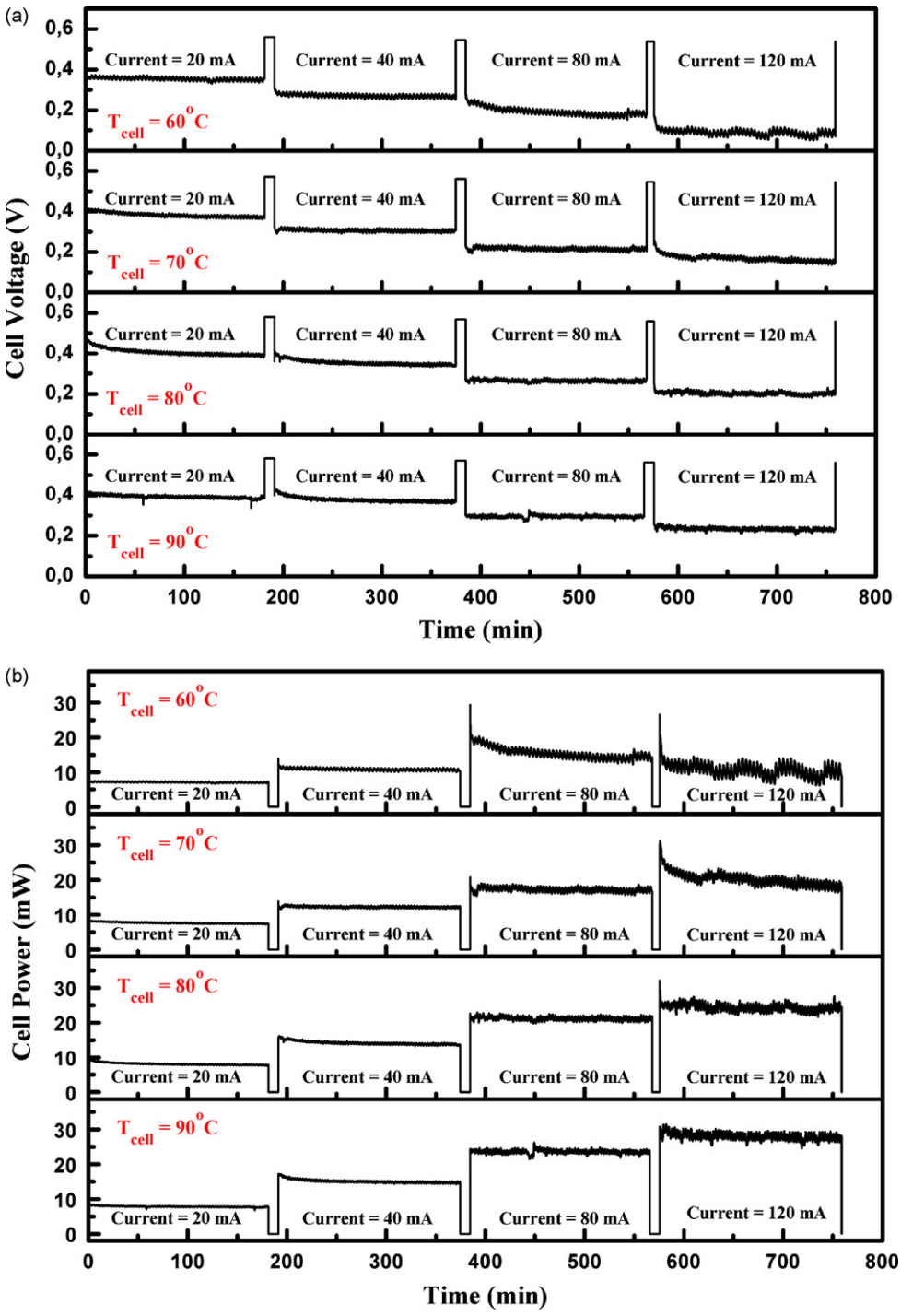

Fig. 4. Galvanostatic operation of the cell: (a) transient response of the cell voltage at different operating discharge current values and different operating temperatures and (b) transient response of the cell power at different operating discharge current values and different operating temperatures.

this time period the cell voltage should not fluctuate significantly in order to avoid a possible change in the reaction mechanism. Furthermore, in order to perform the analysis as effectively as possible the apparatus should be operated under steady state conditions. The time needed for the mixture of the released anode products to be homogeneous within the lines of the experimental apparatus is approximately 10 min. Thus, the first analysis is chosen to be performed after 1 h of the cell operation at a constant discharge current. At each working condition, the concentration of the released anode products has been analysed at least six times for a better quantification. The required retention time for the completion of the each analysis was approximately 20 min. The results of the galvanostatic operation of the cell are shown in Fig. 4(a) and 4(b). At time $t = 0$ min, the cell is operated at a constant discharge current of 20 mA for 3 h. The first GC analyses was performed at time $t = 60$ min. The rest five GC analyses are made periodically every 20 min. After the completion of the six analyses the circuit is opened and it is kept for 10 min. During this period, the lines of the apparatus are cleaned by feeding pure nitrogen at a flow rate of 500 ml min^{-1}. After cleaning the lines, a current of 40 mA is selected and the circuit is closed for another 3 h. The GC analyses are performed as the case of 20 mA. This procedure is repeated at the other

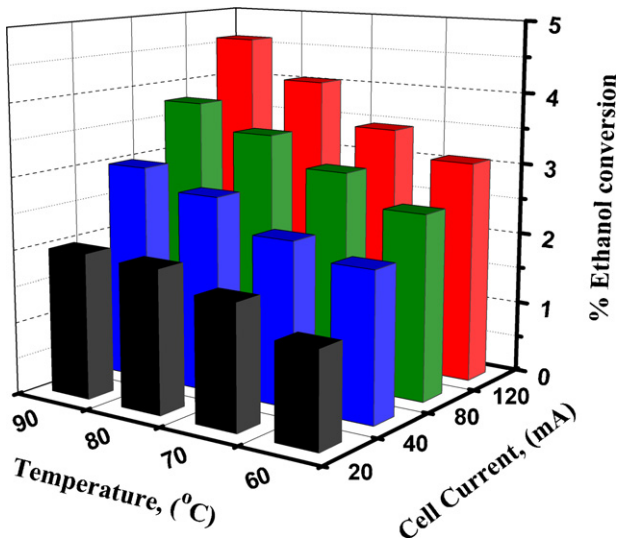

Fig. 5. The effect of the operating discharge cell current and the temperature on the ethanol conversion.

two different discharge current values (80 mA and 120 mA). It can be clearly seen from Fig. 4(a) that, at each temperature, the increase of the current leads to an increase of the overpotential values and consequently a decrease of the operating cell voltage. Moreover, the increase of the temperature results in an increase of the cell voltage when the cell is operated at a constant current. This behavior is explained by the fact that the increase of temperature improves the kinetics of the reactions taking place over the anode and the cathode catalysts, reducing the activation overpotentials. Finally, it should be noted that the cell's voltage fluctuation recorded at a constant current is small (20–30 mV). This is an indication of the following two facts: (a) there is no change of the reaction mechanism during the galvanostatic operation of the cell and (b) the stability of the MEA is very good.

During the galvanostatic operation of the cell, the cell power versus time was also recorded. The corresponding results are presented in Fig. 4(b). It is shown that at three out of four temperatures (70–90 °C) the cell power increases as the cell operating current increase. More precisely, the maximum power is obtained when the current value is 120 mA. Another point that should be also discussed is the effect of the cell discharge current on the cell power fluctuation during the transient measurements. At the lower current values (20 mA and 40 mA), the change of the power is very small, while at the higher current values (80 mA and 120 mA) the change becomes bigger. Especially, when the cell operates at a temperature value of 60 °C and the cell current is 120 mA, the fluctuation of the cell power is obvious during the measurements. The observed behavior at 60 °C could be attributed to the fact that the cell current (120 mA) or 30 mA cm^{-2} is close to the cell's limiting current. Thus, it could be concluded that the observed fluctuations could be possibly attributed to the insufficient reactants transportation over the catalysts. Finally, the effect of the temperature on the cell performance operated under a constant discharge current can be clearly seen. The higher the temperature, the more stable the cell operation is in the effective working temperature range of Nafion®-115 membranes.

3.3. The effect of the cell current and the operating temperature on the ethanol conversion and the products selectivity

The effect of the cell current and the operating temperature on the ethanol conversion is depicted in Fig. 5. It is shown that the increase of the cell current results in an increase of the ethanol conversion when the cell is operated at a constant temperature. The increase of the ethanol conversion is attributed to the fact that the increase of the current load intensifies the ethanol electro-oxidation over the anode catalyst in order to fulfill the current demand [20]. For instance, at 60 °C when the cell current changes from 20 mA to 120 mA, the increase of the ethanol conversion is approximately 135%. At 90 °C the corresponding value is approximately 150%. This could be due to the reason that at higher temperature the oxidation reaction rate is enhanced and thus more efficient fuel utilization is obtained. The maximum value of the ethanol conversion is 4.6% and it has been recorded at 90 °C and 120 mA.

Table 1
Products selectivity as a function of the temperature and the operating cell current.

Current (mA)	% Selectivity AcOH	% Selectivity Acid	% Selectivity CO_2
Temperature (90 °C)			
20	49.6	35.4	15
40	48.8	35.2	16
80	54.7	35.1	10.2
120	56.8	35	8.2
Temperature (80 °C)			
20	45.7	39.4	14.9
40	51.8	35.7	12.5
80	59.6	31.8	8.6
120	65	28	7
Temperature (70 °C)			
20	49	38.7	12.3
40	57.7	33.5	8.8
80	63.7	31.3	5
120	68.8	22.9	8.3
Temperature (60 °C)			
20	52.6	41.9	5.5
40	56.6	37.6	5.8
80	65.2	29.7	5.1
120	66.2	27.6	6.2

The released products detected during the cell operation are acetaldehyde, acetic acid and CO_2. These products are formed according to the previously mentioned (r1)–(r3) reactions.

The selectivity of the released products depends on both cell current and operating temperature. The exact values of the products selectivity at different operating conditions are calculated and summarized in Table 1. It is found that the main product released during the ethanol oxidation over the anode PtRu/C catalyst is acetaldehyde. Its selectivity varies from 45% up to 70% depending on the operating conditions. Acetic acid is also detected and its selectivity varies from 28% up to 42%. Finally, the last product detected in small quantities is CO_2. As far as the products selectivity is concerned, it can be concluded that the increase of the cell discharge current at a constant temperature provokes an increase of the acetaldehyde selectivity and a decrease of the acetic acid selectivity. The same effect of the cell current on the selectivity of the two main products has also been reported in the case of ethanol oxidation over Pt-based electrocatalysts [27,33,34]. According to the literature, the value of the cell voltage favors either the reaction (r1) or the reaction (r2). More precisely, ethanol electro-oxidation towards acetaldehyde is favored at high currents or low cell voltage values. On the contrary, ethanol electro-oxidation towards acetic acid is favored at low currents or higher cell voltage values.

3.4. The effect of the cell current and the operating temperature on the reaction yield

In Fig. 6 the effect of the cell current and the operating temperature on the reaction yield towards each product is depicted. The maximum yield is recorded in the case of ethanol electro-oxidation towards acetaldehyde then is the yield towards acetic acid and

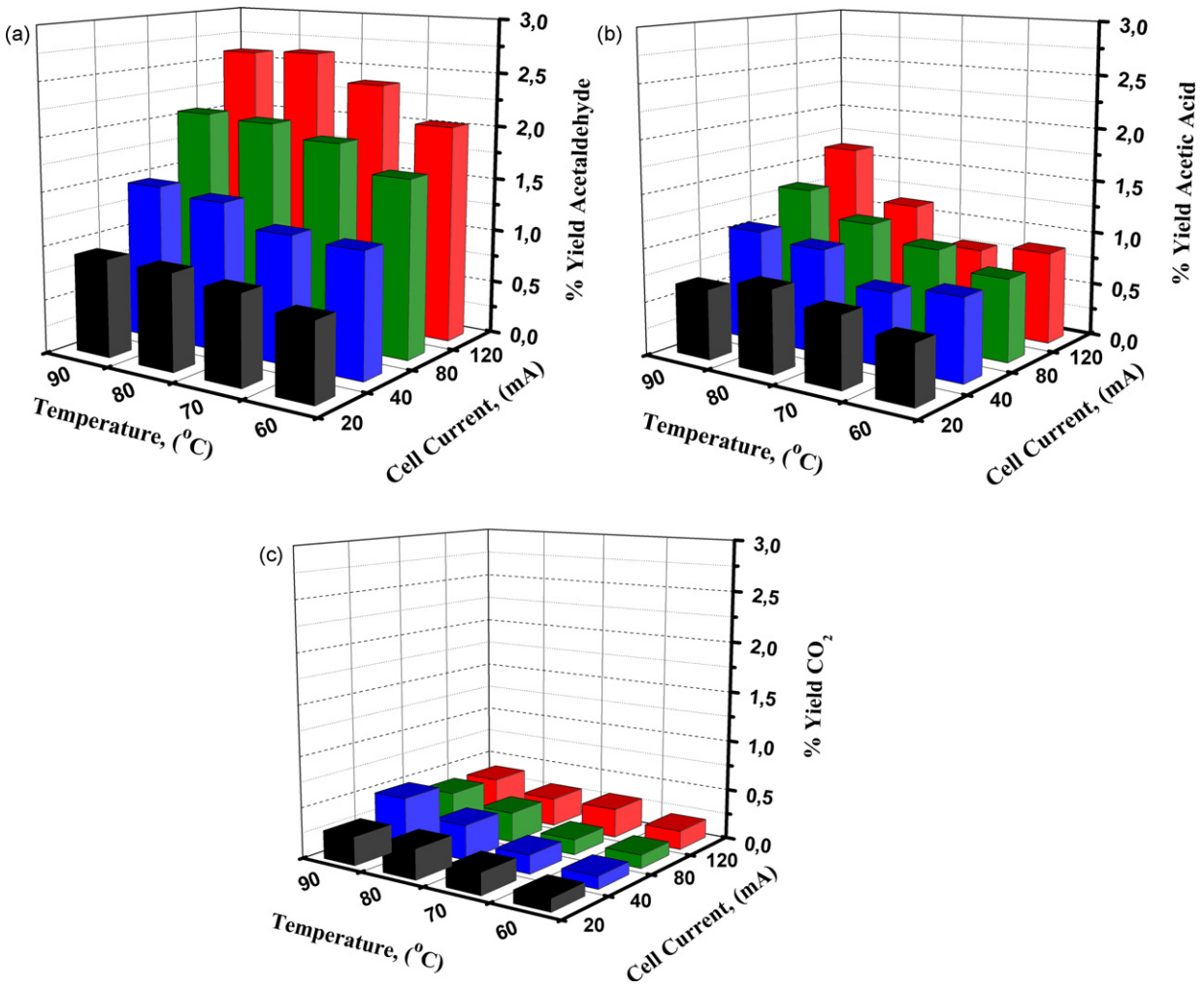

Fig. 6. The effect of the operating discharge cell current and the operating temperature on the reaction yield towards (a) acetaldehyde, (b) acetic acid, and (c) CO_2.

the smallest yield is the one towards CO_2. At a constant temperature, the increase of the operating current results in an increase of the reaction yield towards acetaldehyde and acetic acid. More precisely, at 90 °C as the cell discharge current increases from 20 mA up to 120 mA, the acetaldehyde and the acetic acid yield values are increased approximately by 190% and 150%, respectively. Furthermore, when the cell is operated at a constant current, the increase of the temperature leads to an increase of the reaction yield towards each product. The maximum yield values are found equal to 2.6% for the acetaldehyde, 1.7% for acetic acid, and 0.5% for CO_2 at 90 °C. It should be noted that the above yield values are expected to be small, taking into account the low values of the ethanol conversion reported in the previous paragraph. Moreover, it is known that the thermodynamic conversion of ethanol towards CO_2 at 90 °C is ~10%. Consequently, it can be concluded that the ethanol electro-oxidation towards CO_2 over the examined anode PtRu/C catalyst is not favored.

3.5. Arrhenius plots based on the products formation rates

The Arrhenius plots based on the products formation rates at a cell current of 40 mA are presented in Fig. 7. As it can be seen, the formation rate of the acetaldehyde is the highest one, indicating that the acetaldehyde formation is favored in comparison with the others. The same conclusion could be drawn based on the values of the apparent activation energies. More precisely, the apparent activation energies for each product formation are as follows: 10.3 kJ mol^{-1} in the case of acetaldehyde, 14.5 kJ mol^{-1} in the case of acetic acid, and 50.7 kJ mol^{-1} in the case of CO_2. Based on the above activation energies, it can be concluded once more that the complete ethanol electro-oxidation is not favored over the anode

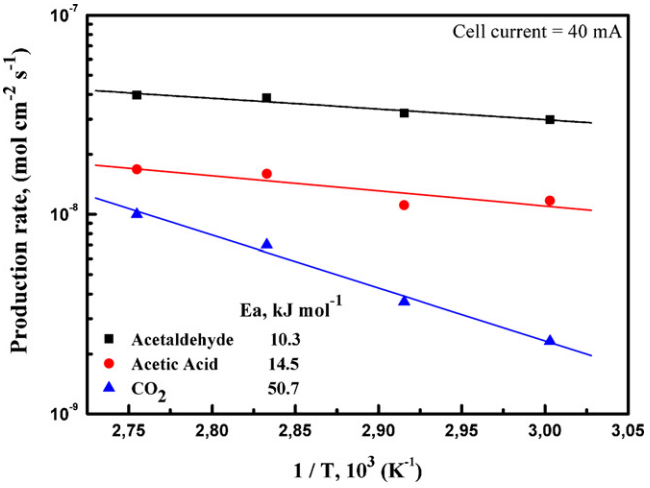

Fig. 7. Arrhenius plots based on the products formation rates at a cell discharge current of 40 mA.

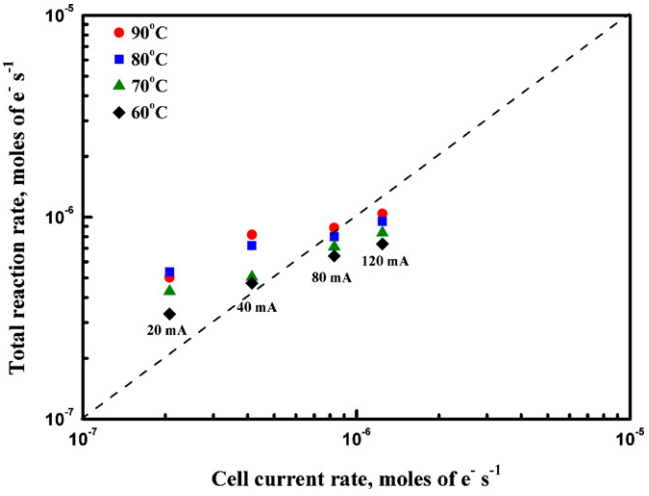

Fig. 8. Comparison between the total reaction rate based on the detected products and the cell discharge current rate.

catalyst. Taking into account also the relatively low values of the reaction yield towards CO_2, it is obvious why the cell power density values are low.

3.6. Comparison between the total reaction rate and the cell current rate

The comparison between the electro-oxidation reactions rate in terms of moles of electrons released per second (mol of $e^- s^{-1}$), based on the detected products and the rate of electrons for the cell's discharge current (in terms of mol of $e^- s^{-1}$) is depicted in Fig. 8. The electro-oxidation reactions rate based on the detected products is calculated from reactions (r1)–(r3).

The rate of electrons based on the operating cell current, r_{cc} could be calculated through the following equation:

$$r_{cc} = \frac{I}{F} \quad (8)$$

where I is the cell discharge current (A) and F the Faraday constant (Cb mol^{-1}).

The dashed line in Fig. 8 indicates the ideal case, where the rate of electrons released through the electro-oxidation reactions equals to the rate of the electrons required for the cell discharge current. It can be clearly seen from Fig. 8 that there is a relatively good agreement between these two rates. More precisely, at low current values (20 mA and 40 mA), the rate of electrons released from the electro-oxidation reactions (based on the detected products) is higher than the rate of electrons from the cell discharge current. This difference could be attributed to the fact that part of the electro-oxidation reactions takes place in gas phase. At a cell discharge current of 120 mA, the rate of electrons released through the electro-oxidation reactions is lower than the corresponding rate of the electrons required for the cell discharge current. This difference could be explained as follows. At higher currents the acetic acid concentration is increased and it could react with ethanol forming small quantities of ethyl acetate according to the following reaction:

$$CH_3CH_2OH + CH_3COOH \rightarrow CH_3COOCH_2CH_3 + H_2O \quad (r4)$$

During the above reaction there are no electrons released. Consequently, in the case that ethyl acetate is formed the rate of moles of electrons per second based on the detected products is lower than the rate of electrons required for the cell current produced. A similar conclusion has also been reported in the literature during the reaction products distribution in a DEFC over Pt-based anode catalysts [14].

4. Conclusions

In the present work the on-line qualitative and quantitative product analysis during a DE-PEMFC was performed. The effect of both cell current and operating temperature on the ethanol conversion, the reaction products selectivity and the reaction yield towards each product was examined. It was found that the ethanol conversion increases as the cell current and the operating temperature increase. The maximum ethanol conversion was found equal to 4.6% when the cell current was 120 mA and the cell temperature was 90 °C. The products released during the fuel cell operation were acetaldehyde, acetic acid and small amounts of CO_2. It was found that the increase of the temperature results in (i) an increase of the acetaldehyde selectivity and (ii) a decrease of the acetic acid selectivity when the cell operates at a constant current. Furthermore, the reaction yield towards each released product was increased as the operating current and the operating temperature were increased. The maximum reaction yield towards acetaldehyde and acetic acid was found 2.6% and 1.7%, respectively, at 90 °C and 120 mA. The maximum value of the reaction yield towards CO_2 was 0.5%, indicating that the C–C bond breakage is difficult to be obtained during the ethanol electro-oxidation over the PtRu/C catalyst. Finally, the above findings were in good agreement with the activation energies calculated from the products formation rates.

Acknowledgements

This work has been supported by the 03ED897 research project, implemented within the framework of the "Reinforcement Programme of Human Research Manpower" (PENED) and co-financed by National and Community Funds (25% from the Greek Ministry of Development – General Secretariat of Research and Technology and 75% from EU-European Social Fund), the Project of NSFC (20903122), the Specialized Research Fund for the Doctoral Program of Higher Education (20070558062).

References

[1] E. Antolini, J. Power Sources 170 (2007) 1–12.
[2] S. Song, P. Tsiakaras, Appl. Catal. B: Environ. 63 (2006) 187–193.
[3] E. Antolini, F. Colmati, E.R. Gonzalez, Electrochem. Commun. 9 (2007) 398–404.
[4] E. Antolini, F. Colmati, E.R. Gonzalez, J. Power Sources 193 (2009) 555–561.
[5] F. Colmati, E. Antolini, E.R. Gonzalez, J. Power Sources 157 (2006) 98–103.
[6] H. Hitmi, E.M. Belgsir, J.M. Leger, C. Lamy, R.O. Lezna, Electrochim. Acta 39 (1994) 407–415.
[7] L. Jiang, G. Sun, Z. Zhou, W. Zhou, Q. Xin, Catal. Today 93–95 (2004) 665–670.
[8] L. Jiang, H. Zang, G. Sun, Q. Xin, Chin. J. Catal. 27 (2006) 15–19.
[9] K.B. Kokoh, F. Hahn, E.M. Belgsir, C. Lamy, A.R. de Andrade, P. Olivi, A.J. Motheo, G. Tremiliosi-Filho, Electrochim. Acta 49 (2004) 2077–2083.
[10] A. Kowal, M. Li, M. Shao, K. Sasaki, M. Vukmirovic, J. Zhang, N. Marinkovic, P. Liu, A. Frenkel, R. Adzic, Nat. Mater. 8 (2009) 325–330.
[11] C. Lamy, S. Rousseau, E.M. Belgsir, C. Coutanceau, J.M. Leger, Electrochim. Acta 49 (2004) 3901–3908.
[12] H. Li, G. Sun, L. Cao, L. Jiang, Q. Xin, Electrochim. Acta 52 (2007) 6622–6629.
[13] Y. Paik, S.S. Kim, O.H. Han, Electrochem. Commun. 11 (2009) 302–304.
[14] S. Rousseau, C. Coutanceau, C. Lamy, J.M. Leger, J. Power Sources 158 (2006) 18–24.
[15] G. Tremiliosi-Filho, E.R. Gonzalez, A.J. Motheo, E.M. Belgsir, J.M. Leger, C. Lamy, J. Electroanal. Chem. 444 (1998) 31–39.
[16] P.E. Tsiakaras, J. Power Sources 171 (2007) 107–112.
[17] F.J.R. Varela, O. Savadogo, J. Electrochem. Soc. 155 (2008) B618–B624.
[18] F. Vigier, C. Coutanceau, F. Hahn, E.M. Belgsir, C. Lamy, J. Electroanal. Chem. 563 (2004) 81–89.
[19] H.F. Wang, Z.P. Liu, J. Am. Chem. Soc. 130 (2008) 10996–11004.
[20] Q. Wang, G.Q. Sun, L. Cao, L.H. Jiang, G.X. Wang, S.L. Wang, S.H. Yang, Q. Xin, J. Power Sources 177 (2008) 142–147.
[21] W. Zhou, Z. Zhou, S. Song, W. Li, G. Sun, P. Tsiakaras, Q. Xin, Appl. Catal. B: Environ. 46 (2003) 273–285.
[22] W.J. Zhou, W.Z. Li, S.Q. Song, Z.H. Zhou, L.H. Jiang, G.Q. Sun, Q. Xin, K. Poulianitis, S. Kontou, P. Tsiakaras, J. Power Sources 131 (2004) 217–223.

[23] W.J. Zhou, S.Q. Song, W.Z. Li, Z.H. Zhou, G.Q. Sun, Q. Xin, S. Douvartzides, P. Tsiakaras, J. Power Sources 140 (2005) 50–58.
[24] W.J. Zhou, B. Zhou, W.Z. Li, Z.H. Zhou, S.Q. Song, G.Q. Sun, Q. Xin, S. Douvartzides, M. Goula, P. Tsiakaras, J. Power Sources 126 (2004) 16–22.
[25] M. Zhu, G. Sun, H. Li, L. Cao, Q. Xin, Chin. J. Catal. 29 (2008) 765–770.
[26] M. Zhu, G. Sun, Q. Xin, Electrochim. Acta 54 (2009) 1511–1518.
[27] C. Lamy, A. Lima, V. LeRhun, F. Delime, C. Coutanceau, J.-M. Leger, J. Power Sources 105 (2002) 283–296.
[28] Q. Wang, G.Q. Sun, L.H. Jiang, Q. Xin, S.G. Sun, Y.X. Jiang, S.P. Chen, Z. Jusys, R.J. Behm, Phys. Chem. Chem. Phys. 9 (2007) 2686–2696.
[29] X.H. Xia, H.D. Liess, T. Iwasita, J. Electroanal. Chem. 437 (1997) 233–240.
[30] H. Wang, Z. Jusys, R.J. Behm, J. Power Sources 154 (2006) 351–359.
[31] S. Song, Y. Wang, P.K. Shen, J. Power Sources 170 (2007) 46–49.
[32] S. Song, W. Zhou, J. Tian, R. Cai, G. Sun, Q. Xin, S. Kontou, P. Tsiakaras, J. Power Sources 145 (2005) 266–271.
[33] C. Lamy, E.M. Belgsir, J.M. Leger, J. Appl. Electrochem. 31 (2001) 799–809.
[34] D.D. James, D.V. Bennett, G. Li, A. Ghumman, R.J. Helleur, P.G. Pickup, Electrochem. Commun. 11 (2009) 1877–1880.